Pergamon

0301-9322(93)E0026-2

Int. J. Multiphase Flow Vol. 20, No. 3, pp. 505–513, 1994

0301-9322/94 $7.00 + 0.00

LOCAL ENHANCEMENT OF HEAT TRANSFER IN A PARTICULATE CROSS FLOW—II

EXPERIMENTAL DATA AND PREDICTED TRENDS

D. B. MURRAY

Department of Mechanical Engineering, Trinity College, University of Dublin, Dublin 2, Ireland

(Received 5 October 1992; in revised form 30 November 1993)

Abstract—Results from an experimental investigation of the effect of solid particles on heat transfer at the first row of a staggered tube array in cross flow are compared with those determined for equivalent conditions from correlations derived previously by the author. Comparison of the experimental data with the predicted levels of heat transfer enhancement from a range of heat transfer mechanisms suggests that the transport of thermal energy by rebounding particles is responsible for much of the measured increase in heat transfer. The total enhancement based on this model of the suspension flow compares well with the experimental data for particles of 46 and 58 μm dia, although the agreement is not as good for 127 μm dia particles. The fine particle model of suspension flow gives levels of enhancement of the correct order for some flow conditions but fails to predict the effect of Reynolds number and particle size. In the light of these results, the suspension heat transfer mechanisms for tubes in cross flow are re-assessed and the dominant effects on enhancement are identified for specific flow conditions.

Key Words: gas–particle cross flow, heat transfer enhancement, particle rebounds, increased thermal capacity, turbulence modification

1. INTRODUCTION

The heat transfer performance of tubes in a particulate cross flow has formed the basis of a number of experimental investigations. For tubes located within a gas fluidized bed, the review of Saxena *et al.* (1978) established that very high heat transfer coefficients are generally associated with in-bed heat transfer surfaces. Improved heat transfer characteristics have also been observed by Wood *et al.* (1980) for tubes located in the splash zone immediately above a fluidized bed and by Byam *et al.* (1981) and George & Grace (1982) for various positions within the freeboard region above the bed. The heat transfer performance of a tubular heat exchanger subject to a cross flow of graphite particles suspended in carbon dioxide was investigated by Woodcock & Worley (1966) for a tightly spaced in-line configuration. For a staggered tube array in cross flow, the effect of glass beads suspended in air on heat transfer was investigated by Murray & Fitzpatrick (1991), while an equivalent study was carried out by Sterritt & Murray (1992) for a square tube configuration.

Although these investigations have taken place, most of the published data are unsuitable for validation of the heat transfer mechanisms identified in part I of this study (Murray 1994, pp. 505–513). The results from fluidized bed investigations relate to high particle concentrations and cannot be used for assessing dilute particulate cross flows. The measurements of Woodcock & Worley (1966) were concerned solely with changes in the overall heat transfer coefficients for a complete heat exchanger. Local heat transfer measurements were obtained by Murray & Fitzpatrick (1991) and by Sterritt & Murray (1992) for tubes in staggered and in-line arrays, respectively, but the range of flow parameters was limited. In addition, considerable uncertainty surrounds the estimates of local solids concentrations and residence times for locations within a tube bank.

This paper compares new experimental data for heat transfer over the front of a tube in the first row of a tube array in cross flow with the predicted enhancement for the same conditions. Comparison of the calculated trends with the experimental data for a range of flow parameters is used to assess the validity of the proposed enhancement mechanisms.

2. CORRELATIONS FOR LOCAL ENHANCEMENT

The local increase in Nusselt number over the front of a tube in a suspension cross flow with large particles may be estimated from [1a, b], whereas the equivalent increase for a flow with very fine suspended solids may be determined from [2]. The derivation of these equations has been described in part I (Murray 1994). In [1a], the direct calculation of the particle rebound mechanism is denoted by the subscript pr1 and the indirect calculation using equivalent turbulence intensities is denoted by pr2 in [1b]. The subscripts itc, Re and *Tu* refer to changes in heat transfer due to the increased thermal capacity of the suspension, the higher effective Reynolds number of the flow and turbulence modification by the particles, respectively:

$$\left(\frac{Nu_{su}}{Nu_a}\right)_{total_{lp}} = 1 + \left[\left(\frac{Nu_{su}}{Nu_a}\right)_{pr1} - 1\right] + \left[\left(\frac{Nu_{su}}{Nu_a}\right)_{Tu} - 1\right] \quad [1a]$$

$$\left(\frac{Nu_{su}}{Nu_a}\right)_{total_{lp}} = 1 + \left[\left(\frac{Nu_{su}}{Nu_a}\right)_{pr2} - 1\right] + \left[\left(\frac{Nu_{su}}{Nu_a}\right)_{Tu} - 1\right] \quad [1b]$$

and

$$\left(\frac{Nu_{su}}{Nu_a}\right)_{total_{fp}} = \left(\frac{Nu_{su}}{Nu_a}\right)_{itc} \times \left(\frac{Nu_{su}}{Nu_a}\right)_{Re} \times \left(\frac{Nu_{su}}{Nu_a}\right)_{Tu}; \quad [2]$$

subscripts lp and fp refer to large and fine particle suspensions, respectively.

3. EXPERIMENTAL FACILITIES AND PROCEDURES

The heat transfer measurements were carried out in a closed-loop circulating wind tunnel with a particle feed and collection system as shown in figure 1. All results reported here were obtained from a tube located at the centre of the first row of a 60° triangular tube array with a pitch-to-diameter ratio of 2. Nine rows and four columns of 25 mm dia, 250 mm length tubes were used, with half-tubes fixed to the side walls to prevent bypass. An individual instrumented and electrically heated tube was used for the heat transfer measurements. The volumetric flow rate through the tunnel was monitored by an orifice plate located on the down leg of the rig.

The solid particles used are spherical glass beads of three size ranges with mass median diameters of 46, 58 and 127 μm. The physical properties of the glass material are as follows: density = 2600 kg/m^3; specific heat = 910 J/kgK; thermal conductivity = 1.4 W/mK. The particles were introduced to the main flow upstream of the test section using an annular jet pump with a conical swirl diffuser to encourage mixing. Downstream of the test section, a cyclone was used to separate the solid particles from the air stream for return to a storage hopper connected to the feed circuit.

Local heat transfer measurements were obtained using a single internally heated thick-walled copper cylinder with a surface-mounted microfoil heat flux sensor (RdF type 27036-1). The sensor was 6 mm wide and 17 mm long with a thickness of 75 μm and was attached to the surface midway along the length of the tube. By rotating the tube through 360° in suitable increments, a profile of the heat transfer around the tube was obtained. A separate thermocouple placed upstream of the tube bank was used to measure the freestream temperature. Heat transfer measurements were taken at 40 equal increments over a full revolution. Data acquisition took place over a 15-s period with a 10-s delay for settling of the flow at each angular position. Data were sampled at a rate of 100 samples per s per channel and all test results were averaged over 3 revolutions, due to some instability of the solids flow. In order to minimize errors due to variations in angular position or solids flow rate, software-controlled stepper motors were used for tube positioning and solids valve opening.

For local heat flux measurements, the experimental uncertainty, quoted by the sensor manufacturers as $\pm 5\%$, is acceptable for the present investigation, as it is the changes in Nusselt numbers, rather than the absolute values, that are of primary interest. Freestream and surface temperature thermometers were calibrated to give an uncertainty of $\pm 2\%$ in the surface-to-air temperature difference, giving an overall uncertainty of $\pm 7\%$ in the absolute local Nusselt number. Individual

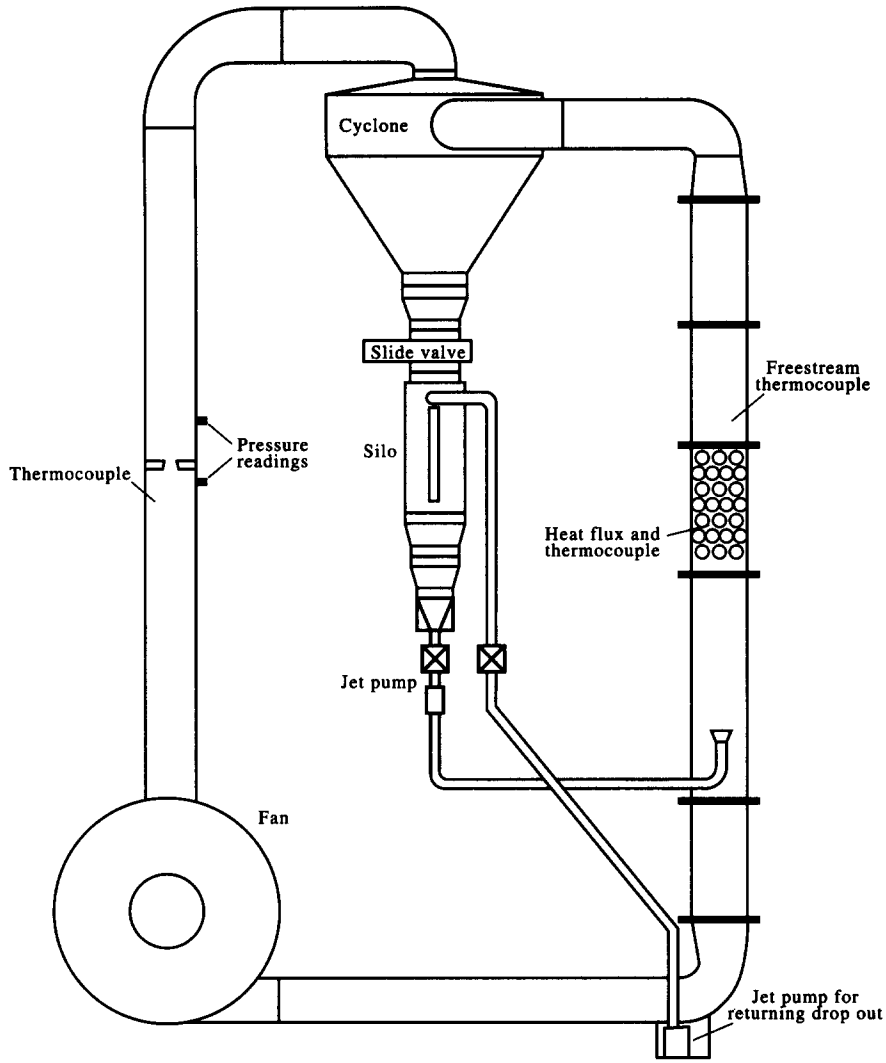

Figure 1. Schematic of the experimental test facility.

local measurements were, however, repeatable to within $\pm 2\%$ for the single-phase Nusselt numbers. For measurements with the suspension flow, variations in the solids flow rate occurred for nominally identical conditions, even with the automated valve opening. The resultant uncertainty in the solids mass loading ratio is of the order of $\pm 20\%$.

A detailed description of the instrumented tube has been given by Murray & Fitzpatrick (1988) and a comparison of data from single-phase tests indicated good agreement with the available published data. Specific details of the suspension flow facility and data logging and analysis procedures have been given by Humphreys (1993).

4. SUSPENSION FLOW CONDITIONS

Two sets of heat transfer data from the first row of the staggered tube array are available for comparison with the enhancement predicted from [1a, b] and [2]. The results of Humphreys (1993) were obtained for flow Reynolds numbers of 3000 and 10,000, with glass beads of mass median dia 46 and 58 μm and with bulk mass loading ratios from 0.5 to 2.2 kg/kg. Heat transfer measurements were made by Scholten (1993) at Reynolds numbers of 7000, 10,000 and 14,000 using glass beads of 127 μm mean dia at mass loading ratios of up to 0.9 kg/kg. In addition, further data for the 58 μm beads were obtained by Scholten (1993), although only at the lower solids concentrations. These operating conditions were dictated by the practical limitations of the

experimental facility. Figure 2 shows the variation in local Nusselt number with angular position for a Reynolds number of 10,000 with 127 μm particles at two mass loading ratios. Although measurements were obtained over the full tube circumference for all tests, the present investigation is concerned only with changes in heat transfer over the front of the tube.

In order to determine which of the proposed models of suspension flow is more appropriate for the range of flow parameters under consideration, all experimental data are compared with the predicted increases in heat transfer from both [1a, b] and from [2].

5. COMPARISON OF EXPERIMENTAL AND PREDICTED TRENDS

A summary of the results from the local heat transfer calculations is given in table 1, along with the equivalent experimental data.

Different heat flux sensors were used in the studies of Humphreys (1993) and Scholten (1993) and the results are presented here in uncalibrated form. This accounts for the differences between the single-phase Nusselt numbers for tests carried out at the same Reynolds number. Note also that for the present investigation, the particle Reynolds numbers and sizes are such that the turbulence enhancement from particulate vortex shedding is not anticipated. This is reflected in the values of $(Nu_r)_{Tu}$, which result solely from turbulence suppression associated with eddy–particle interactions.

From table 1, it is evident that a reasonable degree of correspondence exists between the experimental results and the predicted enhancement from [1a] for large particle suspensions. The trends with particle size, mass loading ratio and Reynolds number are well-matched in most cases, although for the tests carried out with the 127 μm particles the experimental data and predicted values differ in magnitude. The main trends that can be identified from table 1 are higher local heat transfer as the solids mass loading ratio is increased, along with a significant reduction in enhancement as both particle size and flow Reynolds number are increased.

Figure 3 shows the measured and predicted variation in enhancement with increasing mass loading ratio for the 58 μm suspension at a Reynolds number of 10,000. It is clear that, despite some variability in the experimental data, the predicted increases in Nusselt number from [1a] compare well with the measured heat transfer values. The predicted values from [2], for fine particle suspensions, also show levels of enhancement of approximately the correct order. However, the total increases in heat transfer based on the equivalent turbulence intensity calculation of the particle rebound effect are an order of magnitude lower than the measured enhancement, suggesting that the direct calculation of energy transport by rebounding particles is more appropriate. The differences between the measured data from the two sets of experiments at comparable conditions

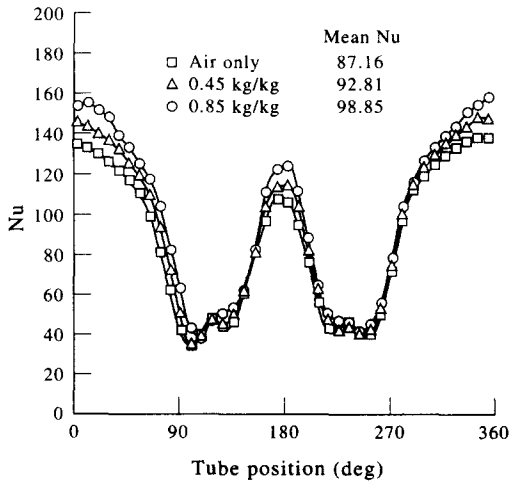

Figure 2. Suspension and single-phase Nusselt numbers (Nu). First row; Re = 10,000, d_p = 127 μm.

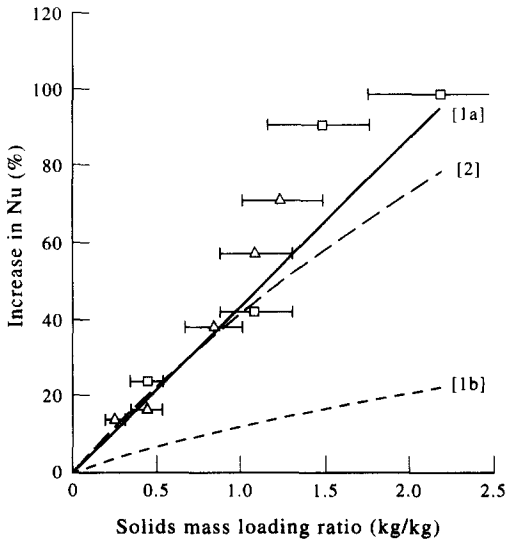

Figure 3. Variation in the local enhancement (increase in Nu) with the mass loading ratio. Re = 10,000, d_p = 58 μm.

Table 1. Comparison of local heat transfer calculations with experimental data for a tube in the first row of a staggered array

Test	Re	S_L (kg/kg)	d_p (μm)	$(Nu)_{a\ exp}$	$(Nu)_{r\ exp}$	$T_{p\ max}$	η_t	$(Nu)_{r\ itc}$	q''_{pr} (W/m^2)	Tu_{eq}	$(Nu_r)_{pr1}$	$(Nu_r)_{pr2}$	$(Nu_r)_{Re}$	$(Nu_r)_{Tu}$	$(Nu_r)_{1a}$	$(Nu_r)_{1b}$	$(Nu_r)_2$
IH1	3000	0.45	58	69.0	1.36	37.6	0.086	1.013	647	0.035	1.366	1.018	1.204	0.992	1.358	1.01	1.21
IH2	3000	1.1	58	69.0	1.98	37.6	0.086	1.031	1581	0.086	1.893	1.042	1.449	0.982	1.875	1.024	1.467
IH3	10,000	0.45	46	111.0	1.25	35.8	0.027	1.004	904	0.11	1.321	1.095	1.204	0.994	1.315	1.089	1.202
IH4	10,000	1.1	46	111.0	2.20	35.8	0.027	1.01	2209	0.269	1.785	1.20	1.449	0.986	1.771	1.186	1.443
IH5	10,000	0.45	58	111.0	1.24	35.5	0.017	1.003	557	0.069	1.197	1.063	1.204	0.996	1.193	1.059	1.203
IH6	10,000	1.1	58	111.0	1.42	35.5	0.017	1.006	1361	0.169	1.482	1.137	1.449	0.991	1.473	1.128	1.445
IH7	10,000	1.5	58	111.0	1.90	35.5	0.017	1.0085	1857	0.23	1.657	1.176	1.58	0.988	1.645	1.164	1.574
IH8	10,000	2.2	58	111.0	1.98	35.5	0.017	1.012	2723	0.337	1.963	1.237	1.79	0.983	1.945	1.22	1.781
JS1	10,000	0.25	58	121.5	1.14	35.5	0.017	1.0015	309	0.038	1.11	1.036	1.118	0.998	1.108	1.034	1.117
JS2	10,000	0.45	58	121.5	1.17	35.5	0.017	1.003	557	0.069	1.197	1.063	1.204	0.996	1.193	1.059	1.203
JS3	10,000	0.85	58	121.5	1.38	35.5	0.017	1.005	1236	0.131	1.374	1.11	1.36	0.993	1.367	1.103	1.357
JS4	10,000	1.1	58	121.5	1.57	35.5	0.017	1.006	1361	0.169	1.482	1.137	1.449	0.991	1.473	1.128	1.445
JS5	10,000	1.25	58	121.5	1.71	35.5	0.017	1.007	1545	0.192	1.55	1.152	1.5	0.99	1.54	1.142	1.495
JS6	7000	0.45	127	101.6	1.10	35.3	0.01	1.002	176	0.004	1.074	1.003	1.204	0.999	1.073	1.029	1.205
JS7	10,000	0.25	127	133.5	1.04	35.1	0.003	1.0003	52	0.0008	1.019	1.0008	1.118	0.999	1.018	0.9998	1.117
JS8	10,000	0.45	127	133.5	1.07	35.1	0.003	1.0005	94	0.0014	1.034	1.0014	1.204	0.998	1.032	0.9994	1.197
JS9	10,000	0.65	127	133.5	1.10	35.1	0.003	1.0007	136	0.002	1.049	1.002	1.285	0.998	1.048	1.0	1.285
JS10	10,000	0.85	127	133.5	1.15	35.1	0.003	1.001	177	0.0026	1.065	1.0026	1.36	0.998	1.063	1.0006	1.359
JS11	14,000	0.5	127	141.7	1.03	35.05	0.002	1.0003	81	0.0008	1.025	1.001	1.225	0.999	1.024	1.0	1.224
JS12	14,000	0.9	127	141.7	1.07	35.05	0.002	1.0005	146	0.0014	1.045	1.0017	1.378	0.999	1.044	1.0007	1.378

H and S refer to the measurements of Humphreys (1993) and Scholten (1993), respectively, Re is the Reynolds number based on the tube diameter (25 mm) and the maximum gap velocity within the array; d_p is the mean particle diameter; S_L is the bulk solids mass loading ratio; Nu_a is the measured single-phase Nusselt number, averaged over a zone extending for around $\pm 30^\circ$ with respect to the front stagnation point; $(Nu_r)_{itc}$ is the predicted ratio of the suspension to single-phase Nusselt numbers as a result of the increased thermal capacity effect; $(Nu_r)_{pr1}$ and $(Nu_r)_{pr2}$ denote the equivalent ratios from the direct calculation and the equivalent turbulence intensity model, respectively, of the particle rebound mechanism; $(Nu_r)_{Re}$ represents the enhancement associated with the higher effective Reynolds number of the suspension; $(Nu_r)_{Tu}$ refers to the change in the local Nusselt number due to turbulence modification by the particles; $(Nu_r)_{1a}$ is the total enhancement predicted from [1a]; $(Nu_r)_{1b}$ is the total enhancement calculated from [1b]; $(Nu_r)_2$ is the total enhancement derived from [2]; and $(Nu_r)_{exp}$ is the ratio of the measured suspension Nusselt number to that for the single-phase flow, averaged over a zone extending for around $\pm 30^\circ$ with respect to the front stagnation point.

are due to variations in the solids mass loading ratio, as discussed earlier, and error bars are shown to denote the expected range of values.

In figure 4, measured and predicted results for the effect of the solids mass loading ratio on heat transfer for the 127 μm suspension at a Reynolds number of 10,000 are shown. It can be seen that the agreement between the predicted change in Nusselt number from [1a] and the measured increase is not as good as for the 58 μm particles but the trend with increasing mass loading ratio is similar for both cases. The predicted enhancement from [2] is much larger than the measured increase in heat transfer, but also shows that increasing solids concentration will result in higher levels of enhancement.

Figure 5 shows the effect of particle size on Nusselt number for a Reynolds number of 10,000 and a solids mass loading ratio of 0.45 kg/kg. It is evident that the dominant trend is one of increasing enhancement with a decrease in particle size, as predicted from [1a]. In contrast, the curve representing the enhancement derived from [2] for fine particle suspensions fails to model the effect of particle size within the range for which experimental data are available. (Note that the relationship between the solids mass loading ratio and the enhancement of heat transfer, determined from figures 3 and 4, has been used to provide the error bars on figure 5, which relate to the uncertainty in the solids mass loading ratio.)

In figure 6, the effect of varying the Reynolds number is examined for the 58 μm suspension. The data shown are for mass loading ratios of 0.45 and 1.1 kg/kg. In both cases, a trend of increasing enhancement with a reduction in Reynolds number can be identified. For the data shown, the measured heat transfer performance is well-matched by the predicted enhancement from [1a] for large particle suspensions. Equation [2] predicts the same level of enhancement for all Reynolds numbers at a given solids mass loading ratio and is not shown here. Figure 7 shows the effect of Reynolds number on the increase in Nusselt number for the 127 μm suspension. Once more, increasing Reynolds number leads to a reduction in the level of enhancement. In this case, the agreement between the measured and predicted enhancement from [1a] is not close but the relative trends are similar. The error bars shown on figures 6 and 7 also originate in the uncertainty in the solids mass loading ratio.

6. DISCUSSION

In figures 3–7, comparison of the total enhancement predicted from [1a, b] and [2] with the experimental data suggests that the large particle model of the suspension flow, with direct calculation of the thermal energy transport by rebounding particles, is most appropriate for predicting the heat transfer performance of gas–particle suspensions in cross flow. This is valid for

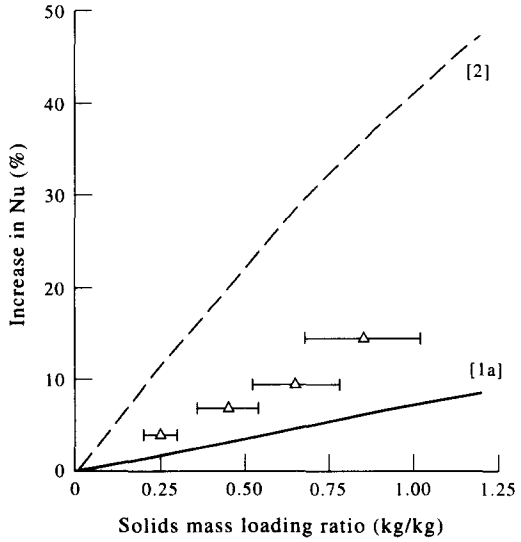

Figure 4. Variation in the local enhancement (increase in Nu) with the mass loading ratio. Re = 10,000, d_p = 127 μm.

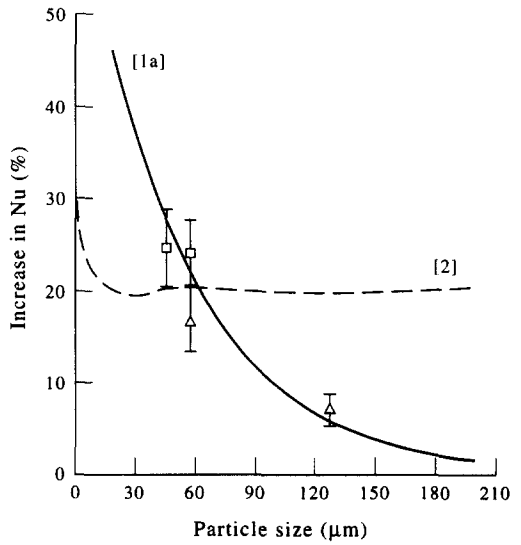

Figure 5. Variation in the local enhancement (increase in Nu) with particle size Re = 10,000, S_L = 0.45 kg/kg.

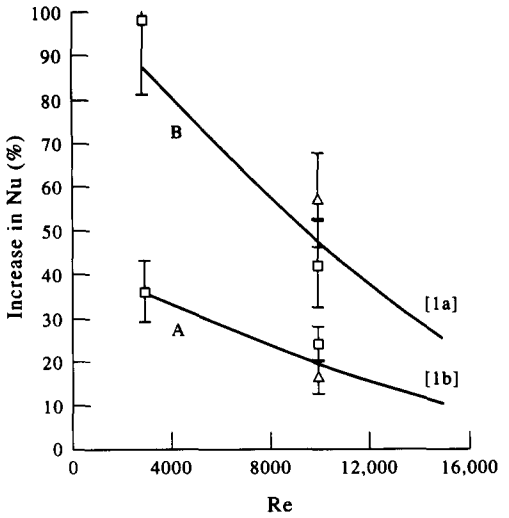

Figure 6. Variation in the local enhancement (increase in Nu) with Reynolds number (Re). (A) $d_p = 58\ \mu m$, $S_L = 0.45$ kg/kg; (B) $d_p = 58\ \mu m$, $S_L = 1.1$ kg/kg.

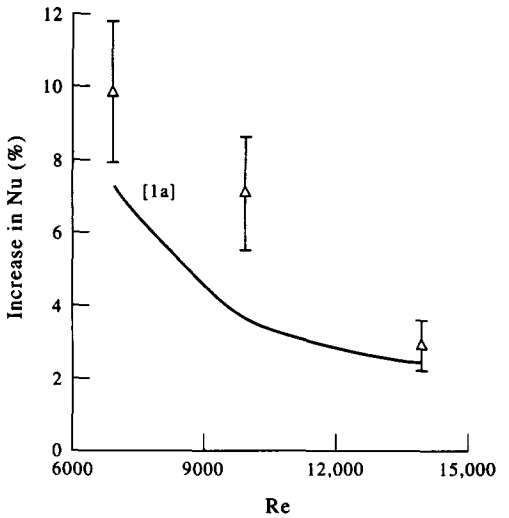

Figure 7. Variation in the local enhancement (increase in Nu) with Reynolds number (Re). $d_p = 127\ \mu m$; $S_L \simeq 0.45$ kg/kg.

the range of flow parameters under consideration. Although the enhancement resulting from individual heat transfer mechanisms has not been shown in these graphs, it can be determined readily from table 1 that the dominant influences on heat transfer are the particle rebound mechanism for [1a, b] and the effective Reynolds number term for [2]. Thus, the enhancement anticipated solely from the increased thermal capacity effect is low, due to the short time available to particles to participate in the heat transfer process, and the expected contribution to this effect from particle-to-wall conduction is extremely small and is not listed separately. In addition, the reduction in heat transfer resulting from turbulence suppression by the particles is generally modest.

Although the enhancement calculated solely from the increased thermal capacity effect is very low, the measured increase in heat transfer with a reduction in particle size appears to originate in this effect as smaller particles can more easily utilize their high heat capacity. Clearly, the trend with particle size is linked to the increased thermal capacity of the suspension, but the direct transport of stored thermal energy out of the heated fluid zone by rebounding particles is responsible for most of the increase from this effect. Note that although the thermal effectiveness factor is small in all cases, suggesting a modest increase in particle temperature, the large number of particle rebounds, together with the high heat capacity of the particles, means that a high degree of enhancement is predicted from the direct calculation of the particle rebound effect. For the limiting case of infinitesimally small particles, the suspension will behave like a homogeneous fluid and will have the maximum thermal effectiveness factor of 1. In this case, there will be no contribution from particle rebounds but instead the higher effective density, and hence the Reynolds number, of the flow will influence heat transfer by means of a reduction in the local boundary-layer thickness. This limiting condition can be calculated from [2] and is shown in figure 5. For large particle suspensions, the change in boundary-layer characteristics associated with a homogeneous fluid of higher density is not anticipated. Thus, the effective Reynolds number term, which represents this mechanism and which suggests a uniform level of enhancement irrespective of particle size, is invalid. As mentioned in part I (Murray 1994), it is possible that inertial effects associated with the motion of large particles could lead to a localized generation of turbulence close to the tube surface. However, the low measured enhancement for the 127 μm particle tests, shown in figure 4, along with the low particle Reynolds numbers associated with these particles, suggests that this is not the case here. Enhancement from the wall conduction mechanism also increases with a reduction in particle size, but this effect is insignificant for the range of flow parameters under consideration and is included within the increased thermal capacity data of table 1.

It has been shown in figures 6 and 7 that a reduction in Reynolds number leads to an increase in the measured levels of heat transfer enhancement. From table 1, it is evident that the variation in enhancement with Reynolds number can again be attributed to thermal capacity and particle

rebound considerations. The reduction in enhancement with increasing Reynolds number is mainly due to shorter particle residence times, as an increase in Reynolds number reduces the extent of the heated fluid zone and also leads to higher particle velocities. This causes a reduction in the thermal effectiveness factor and a consequent decrease in the enhancement from the increased thermal capacity effect and, more significantly, from the particle rebound mechanism. The contribution from particle-to-wall conduction rises with increasing Reynolds number, but this effect is too small to influence the measured changes in heat transfer.

In part I (Murray 1994) it was suggested that for fine particle suspensions, whose behaviour approximates that of a homogeneous fluid, the increases in heat transfer due to the higher heat capacity and higher effective density of the suspension would be linked. Any change in heat transfer resulting from turbulence modification by the particles would also interact with the physical properties of the suspension. As a consequence, a multiplicative relationship exists between the individual enhancement terms in [2]. For large particle suspensions, the enhancement associated with the thermal energy transport by rebounding particles is expected to be independent of changes in the heat transfer due to gas–particle turbulent interactions and thus the two terms are linked by an additive relationship in [1a, b]. In this analysis, the particle rebound mechanism is considered to encompass the enhancement associated with the increased thermal capacity effect. Hence, no increased thermal capacity term appears in [1a, b], even though this mechanism is ultimately responsible for most of the predicted enhancement of heat transfer. Likewise, increases in heat transfer resulting from particle-to-wall conduction form an integral part of the increased thermal capacity calculation.

Although the general validity of [1a, b] and [2] can be established by comparison of the experimental data with the predicted increases in heat transfer, it is not possible to confirm the degree of dependence between the separate heat transfer mechanisms. This is because [1a, b] and [2] each have one dominant term, meaning that similar values for the total enhancement are obtained regardless of whether the individual terms are added or multiplied. Nevertheless, the justification for treating fine and large particle suspensions in different ways is considered to be valid.

Some aspects of this analysis are clearly approximate and accurate predictions of heat transfer enhancement cannot be expected. In particular, the use of an equivalent turbulence intensity to model the particle rebound mechanism is speculative and has been shown here to significantly underpredict the measured increase in heat transfer. Thus, [1b] is not suitable for the prediction of enhancement in gas–particle cross flows. Likewise, the increases in heat transfer predicted from [2] do not reflect the measured trends with Reynolds number and particle size, suggesting that this equation may only be valid for very fine particle suspensions which closely approximate homogeneous flows. The estimate of residence time is still inexact and it is difficult to quantify the effect on heat transfer of changes in the flow structure due to the movement of discrete particles. Detailed experimental data on particle trajectories and local residence times are needed to clarify some of these issues and work is planned in this respect. Nevertheless, this analysis represents a logical first stage in the development of a correlation for the local enhancement of heat transfer in suspension cross flows.

7. CONCLUSIONS

The effect of solid particles in suspension on local convective heat transfer over the front of tubes in cross flow has been investigated. From a comparison of experimental data with predicted changes in heat transfer, the main mechanisms of heat transfer enhancement have been identified as:

(1) The transport of thermal energy by rebounding particles.
(2) Changes in the flow structure due to the higher effective Reynolds number of the suspension.

The first mechanism encompasses the increased thermal capacity of the suspension and is always important in influencing heat transfer. Changes in the flow structure due to the physical properties of the mixture are likely to be more significant for fine particle suspensions. Conduction between

impinging particles and the tube wall has been found to have an insignificant effect on heat transfer for the range of flow parameters under consideration, and the influence on heat transfer of turbulence modification by the particles has also been identified as a minor effect. A correlation involving a direct calculation of heat transfer by particle rebounds, with minor contributions from other mechanisms, [1a], has been shown to give good correspondence between predictions and experimental data for the suspension flow conditions of the present investigation.

Acknowledgements—Financial support for the experimental measurements was provided by DGXII of the European Commission under research Grants EN3F/44/IRL and JOUF/31/C (EDB). The heat transfer measurements were made by J. Scholten and I. Humphreys.

REFERENCES

BYAM, J., PILLAI, K. K. & ROBERTS, A. G. 1981 Heat transfer to cooling coils in the splash zone of a pressurized fluidized bed combustor. *AIChE Symp. Ser.* **77**(208), 351–358.

GEORGE, S. E. & GRACE, J. R. 1982 Heat transfer to horizontal tubes in the freeboard region of a gas fluidized bed. *AIChE Jl* **28,** 759–765.

HUMPHREYS, I. 1993 Design, development and testing of an experimental test facility to investigate the heat transfer properties of a two phase gas–solid flow. M.Sc. Thesis, Trinity College, Univ. of Dublin.

MURRAY, D. B. 1994 Local enhancement of heat transfer in a particulate cross flow—I. Heat transfer mechanisms. *Int. J. Multiphase Flow* **20**.

MURRAY, D. B. & FITZPATRICK, J. A. 1988 Local heat transfer coefficients for a tube array using a micro-foil heat flow sensor. In *Proc. 2nd U.K. National Conf. on Heat Transfer*, Glasgow, Vol. 2, pp. 1635–1649.

MURRAY, D. B. & FITZPATRICK, J. A. 1991 Heat transfer in a staggered tube array for a gas–solid suspension flow. *Trans. ASME J. Heat Transfer* **113,** 865–873.

SAXENA, S. C., GREWAL, N. S. & GABOR, J. D. 1978 Heat transfer between a gas fluidized bed and immersed tubes. *Adv. Heat Transfer* **14,** 149–247.

SCHOLTEN, J. 1993 Cross flow heat transfer between a gas-solids suspension and a staggered tube array. Research report, Dept of Mechanical Engineering, Trinity College, Univ. of Dublin.

STERRITT, D. B. & MURRAY, D. B. 1992 Heat transfer mechanisms in an in-line tube bundle subject to a particulate cross flow. *Proc. Instn Mech. Engrs* **206,** 317–326.

WOOD, R. T., KUWATA, M. & STAUB, F. W. 1980 Heat transfer to horizontal tube banks in the splash zone of a fluidized bed of large particles. In *Fluidization* (Edited by GRACE, J. R. & MATSEN, J. M.), pp. 235–242. Plenum Press, New York.

WOODCOCK, M. T. & WORLEY, N. G. 1966 Gas–solid suspensions as heat transfer media. *Proc. Instn Mech. Engrs* **181,** 17–33.